

Dopamine Adsorption on TiO₂ Anatase Surfaces.

I. Urdaneta ^{1,2,3}, A. Keller³, O. Atabek ³, J. L. Palma⁴, D. Finkelstein-Shapiro⁴, T. Pilarisetty⁴, V. Mujica⁴, M. Calatayud ^{1,2,5*}

¹ Sorbonne Universités, UPMC Univ. Paris 06, UMR 7616, Laboratoire de Chimie Théorique,
F-75005, Paris, France

² CNRS, UMR 7616, Laboratoire de Chimie Théorique, F-75005, Paris, France

³ Institut des Sciences Moléculaires d'Orsay (ISMO) Bât 350, UMR8214 CNRS-Université Paris-Sud, Orsay, France

⁴ Department of Chemistry and Biochemistry, Arizona State University, P.O. Box 871604,
Tempe, Arizona 85287, U.S.A

⁵ Institut Universitaire de France

*Corresponding author: Dr. M. Calatayud calatayu@lct.jussieu.fr

Laboratoire de Chimie Théorique

Université P. M. Curie, UMR 7616, PO Box 137

F-75005, Paris, France

Phone : +33 1 44 27 25 05

Fax : +33 1 44 27 41 17

Abstract

The dopamine-TiO₂ system shows a specific spectroscopic response, Surface Enhanced Raman Scattering (SERS), whose mechanism is still unknown. In this study the goal is to reveal the key role of the molecule-nanoparticle interface in the electronic structure by means of *ab initio* modeling. The dopamine adsorption energy on anatase surfaces is computed and related to changes in the electronic structure. Two features are observed: The appearance of a state in the material band gap, and charge transfer between molecule and surface upon electronic excitation. The analysis of the energetics of the systems would point to a selective adsorption of dopamine on the (001) and (100) terminations, with much less affinity for the (101) plane.

Keywords: anatase, charge-transfer mechanism, SERS, Raman, DFT

Introduction

In the past decade much effort has been devoted to the study of TiO₂ nanoclusters because of their multiple applications in chemistry ¹. Considerable attention has been given to the adsorption of organic molecules on TiO₂ clusters, since these systems have shown specific optical properties in dye-sensing or photocatalysis ². Very recently an important increase of the emitted Raman signal has been observed upon adsorption of dopamine on titania nanoparticles (NP) with respect to the bare molecule ³⁻⁹. This phenomenon, known as Surface Enhanced Raman Scattering (SERS), is quite common for metallic supports, but is much less characterized for semiconducting materials. The mechanism explaining the enhancement of the Raman signal in the dopamine-TiO₂ system has been postulated to be one-electron charge transfer ^{10,11}, from the molecule to the nanoparticle. The goal of the present paper is to investigate the interface dopamine-TiO₂ on an atomic level by means of Density Functional Theory (DFT) periodic boundary condition calculations in order to elucidate the features connecting geometrical and electronic structures. It will be shown that the electronic structure of the complex system dopamine-anatase surface is essential to explain the basic features of the observed SERS.

SERS was observed on a series of experiments ^{3,4} for nanoparticles between 2 to 5 nm diameter at different dopamine content, in chloride acid solution at pH=4 for laser excitation wavelengths going from 500 to 800 nm. The adsorption site and strength play a key role in the SERS effect. Experimentally it is known that dopamine adsorbs perpendicular to the TiO₂ surface of the nanoparticle through its oxygen atom which is bonded to a surface Ti site ³. But it is yet unclear if it is a monodentate adsorption (only one dopamine oxygen is linked to one Ti), bidentate adsorption (both oxygen sites linked to adjacent Ti atoms) or chelated

adsorption (both oxygen sites adsorbed on the same Ti). NEXAFS experiments on isolated dopamine and dopamine on anatase TiO_2 (101)¹² and rutile (110)¹³ showed that the molecule interacts strongly with the surface, in agreement with theoretical calculations. Previous studies on catechol interaction with TiO_2 nanoparticles, a hybrid of great importance for solar technologies whose geometry is close to dopamine, pointed out to the crucial role of the adsorption mode of the molecule on the optical properties.¹⁴⁻¹⁷ The experimental and theoretical literature on catechol conclude to the dissociative adsorption of the molecule in a bidentate mode on the rutile (110) anatase (101) surfaces¹³, with easy interconversion to monodentate upon reprotonation¹⁸. Chelated geometries are found to be stable in the presence of defective TiO_2 ¹⁵ although their electronic structure might not result in the formation of a band gap state¹⁹. In the present paper we focus on the adsorption systems of neutral dopamine on a series of anatase surfaces in order to unravel structural and electronic features to explain the observed SERS.

Modeling hybrid systems has been undertaken in the past by considering small TiO_2 nanoclusters (TiO_2)_N $N=2,4,\dots,10$ and one dopamine molecule²⁰⁻²⁴. These investigations indicate that the dopamine effect on the TiO_2 cluster electronic structure is two-fold: first, it gives rise to new occupied states (coming mainly from the molecule) inside the cluster's original band gap, and second it gives rise to a large charge polarization effect involving the HOMO-LUMO orbitals of the complex since the HOMO is localized mainly in the molecule while the LUMO is mostly localized in the nanocluster. The use of small nanoclusters as models for hybrid systems allows considering quantum confinement, which is one of the main reasons for the onset of size-dependent properties in these systems²⁰. However such models might not be directly comparable to the real systems because i) their size is really small, few Å whereas the real nanoparticles are few nm diameter ii) the concentration of

dopamine modeled is high iii) there are many low coordinated atoms in the cluster, much more than in real surfaces, like titanyl Ti=O, three- or four-fold titanium sites. In the present work we use periodic slabs to investigate the geometrical, energetic and electronic features of dopamine on bare anatase surfaces, focusing on molecule-surface behavior that occurs on the atomic level. In such model the excited states form a conduction band instead of discrete states arising from the use of cluster models and therefore bring important complementary information on the electronic structure of dopamine-NP hybrid systems. To the best of our knowledge the use of slab models for the dopamine-anatase system has not been reported yet.

In the present paper, the dopamine adsorption on three different anatase terminations is investigated so as to characterize the effect of the surface topology in the interaction between the molecule and the semiconducting nanoparticle. It will be shown that for the three slabs investigated dopamine chemisorbs following a double deprotonation and forming two O-Ti bonds with two surface Ti sites. However, the dopamine-titania interaction is energetically more favorable for (001) and (100) terminations than for (101) indicating a possible selectivity in the adsorption. The electronic structure of the most stable models shows a molecular state located in the slab TiO_2 band gap whose position depends on the surface termination. Moreover, the excitation to a triplet state show the interaction of the HOMO located in the molecule and the LUMO located in the surface Ti sites. The electronic structure obtained for dopamine adsorbed on anatase slabs is therefore consistent with the charge transfer associated to the SERS effect.

The paper is organized as follows. First, the methods and models used are described. Second, the adsorption modes of dopamine on selected anatase surfaces are presented.

Third, the electronic structure of ground and excited states of selected systems is analyzed.

A section of conclusions closes the paper.

Methods and Models

Calculations are performed using the VASP 5.3.3 code^{25,26} with the Perdew-Becke-Ernzerhof functional²⁷. The core electrons are kept frozen by the plane augmented wave method PAW^{28,29}. The valence electrons (Ti: 4s² 3d², O: 2s² 2p⁴, C: 2s² 2p², N: 2s² 2p⁵, H: 1s¹) are explicitly described by means of a plane-wave basis set with a cutoff at 400 eV. A vacuum of at least 20 Å in the c direction, orthogonal to the slab, is kept in order to prevent interaction between successive slabs, repeated in three dimensions. The reciprocal space was sampled with a Monkhorst-Pack grid adapted to the dimensions of each system, the distance between two k-points in the reciprocal space being \sim 0.05 Å⁻¹. Geometrical optimization is carried out by means of the conjugate-gradient algorithm with a tolerance of 0.1 meV in the total energy; all atoms are allowed to relax. Dipole corrections have been included in the direction perpendicular to the slab.

In order to give a description of the electronic structures, the singlet closed-shell optimized geometry has been chosen as starting point. From this structure a single-point calculation with a 3x3x1 k-points sampling is done to calculate the corresponding density of states (DOS). Then, the excited states are simulated by an excitation of the structure to a triplet ($N_{\alpha,\beta}=2$) state. This approach allows giving an estimate of the relative energy of the electronic states, as well as the contributions of both molecule and slab to the DOS. An analysis of the electron spin density is done to get a picture of the charge transfer occurring upon dopamine adsorption on anatase TiO₂. Since pure GGA functional give an artificial

delocalization of the electron in the triplet excited state, we have conducted these calculations at the GGA+U level i.e. a Hubbard parameter U-J=4 has been included for Ti 3d orbitals to account for the self-interaction error.

As models, three planes of the anatase phase have been considered: (101), (001) and (100), on top of which one dopamine molecule is adsorbed in different configurations. The unit cells have been chosen so as to allow a reasonable coverage of 0.25 molecules per surface titanium sites. Table 1 shows the dimensions of the unit cells chosen. Different orientations of the molecule have been tested. The adsorption energy E_{ads} is calculated as the energy difference between the energy of the adsorption complex, and the sum of the gas-phase molecule and the bare slab. In our convention if the adsorption stabilizes the system, $E_{ads} < 0$. Thus, the more negative the E_{ads} , the more stable the system.

	(001)	(100)	(101)
Unit cell	2x2	2x1	2x2
a in Å	7.57	7.57	7.57
b in Å	7.57	9.51	10.91
c in Å	40	40	40
Slab thickness in Å	13.4	13.8	13.1
composition	Ti ₂₄ O ₄₈	Ti ₃₂ O ₆₄	Ti ₃₂ O ₆₄
E_{ads} in eV	-1.86	-1.14	-0.67

Table 1: geometrical parameters of the slab models and calculated adsorption energy for dopamine adsorption. Each slab model has 4 surface titanium atoms

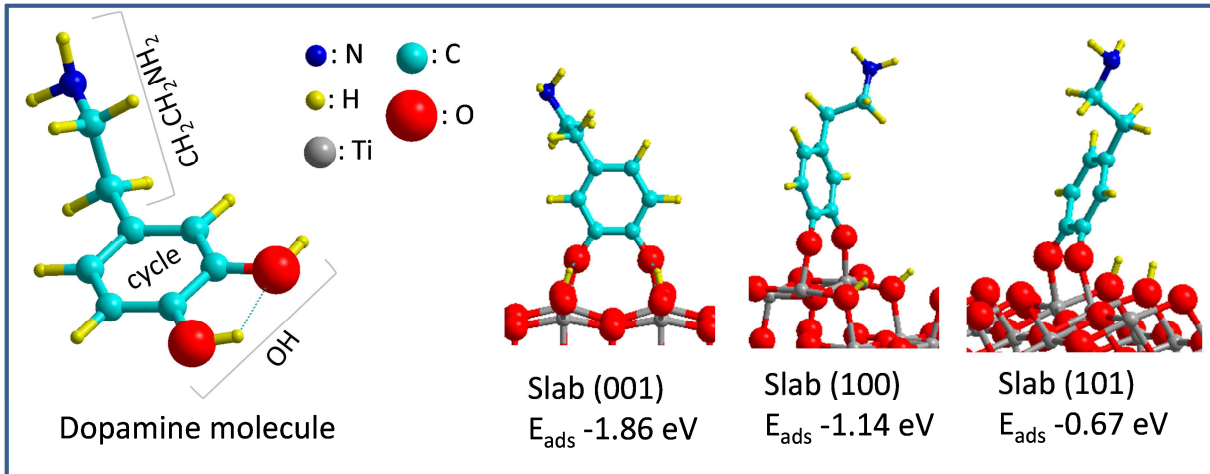


Figure 1: gas-phase dopamine and most stable adsorption systems obtained for the (001), (100) and (101) anatase terminations.

Adsorption systems

Multiple possibilities of dopamine adsorption were considered, and the most stable ones are depicted in Figure 1. Table 1 shows the adsorption energies for each surface orientation. The molecule dissociates by its OH bonds and adsorbs on two under-coordinated Ti sites forming two $\text{Ti}_{\text{surf}}-\text{O}$ and two $\text{O}_{\text{surf}}-\text{H}$ bonds, this is the bidentate mode. Neither the molecular mode i.e. without OH dissociation, nor the partially dissociated modes are found as stable as the fully deprotonated one. Dopamine stays perpendicular to the surface in all cases. The monodentate mode (one oxygen of the molecule on one Ti site, the other as OH group) and the chelated (two oxygen sites of the molecule on one Ti site) evolve during the optimization to the bidentate one for the (001) termination. This mode is suggested as the most stable one in experimental works¹² although in this reference the authors do not discard the

presence of other modes. The adsorption through two oxygen atoms supports theoretical calculations of catechol on anatase TiO_2 by Redfern et al.³⁰. In ref¹⁵, catechol adsorption on (101) periodic slabs gives an adsorption energy of -0.94 eV for a thinner slab model (three TiO_2 bilayers in ref.¹⁵, six TiO_2 bilayers in the present work). Liu et al.¹⁵ report an adsorption energy of -0.70 eV for the catechol bidentate mode at the diluted limit on anatase (101).

As we see from Table 1 and Figure 1, the most favorable adsorption energy is found for the (001) orientation, $E_{\text{ads}} = -1.86$ eV, followed by the (100) with $E_{\text{ads}} = -1.14$ eV. The (101) slab shows $E_{\text{ads}} = -0.67$ eV. These values follow the expected trend of reactivity to molecule adsorption with respect to the bare surface, i.e., the (001) and (100) terminations are more stabilized than the (101) when the molecule adsorbs. This is explained by the lower reactivity of the (101) bare slab which is known to be the most stable. According to our results, dopamine shows a stronger affinity for (001) and (100) planes. Whereas the order of stability for the bare surfaces decreases as (101) > (001) > (100)³¹ the stability of the covered slabs depends on the nature of the adsorbate and the order is substantially different^{32,33}. This is the case for dopamine.

Bader population analysis³⁴ has been carried out for the bidentate adsorption modes of Figure 1, Bader charges for selected atoms are given in Table 2. It can be observed that the dopamine molecule transfers 0.77 |e| (001), 0.81 |e| (100) and 0.82 |e| (101) to the slab upon adsorption in the bidentate mode becoming positively charged. The transferred electrons come mainly from the oxygen atoms, whose charge decreases from -1.83 |e| in the gas-phase to -1.60/-1.69 |e| for the adsorbed systems, and from the aromatic cycle, whose charge passes from +1.64 |e| in the gas-phase to ~+1.90 |e|, see Table 2. The slab becomes thus negatively charged upon adsorption. This extra charge is mainly located on

the surface hydroxyl groups, with an oxygen charge of approx. -1.68 |e| to be compared with the bulk oxygen charge of -1.32 |e|. Also, the surface titanium sites bonded to dopamine exhibit a charge of +2.60/+2.63 |e| which is slightly less positive than the Ti in the bulk charged +2.63/+2.65 |e|.

Regarding the dissociation of the dopamine OH groups, the process obeys an acid-base adsorption mechanism ³⁵ where the surface oxygen sites would be more basic than the molecule ones, inducing the migration of the H⁺ groups to bind to the former. Liu et al. ¹⁵ found energetic barriers for catechol dissociation of 0.45 eV (first deprotonation) and 0.40 eV (second deprotonation) which indicate easy deprotonation and interconversion on the (101) termination, supported by Scanning Tunneling Microscopy observations.

	(001)	(100)	(101)	Gas-phase dopamine
Dopamine	+0.77	+0.81	+0.82	0.00
OH groups	-1.20	-1.15	-1.14	-1.66
Cycle	1.93	1.89	1.91	1.64
CH ₂ CH ₂ NH ₂	0.04	0.07	0.05	0.02
Ti-O-C	-1.60	-1.68	-1.69	-1.83
Slab	-0.77	-0.81	-0.82	
Ti-O-C	+2.60	+2.62	+2.63	
O-H	-1.68	-1.68	-1.69	
Ti _{bulk}	+2.64	+2.63	+2.65	
O _{bulk}	-1.32	-1.32	-1.33	

Table 2: Bader charges for selected atoms and groups of atoms in |e|, models in Figure 1.

Electronic structure: DOS and spin distribution.

The dopamine and slab-projected DOS calculated for the most stable systems found for the three anatase terminations are shown in Figure 2. The calculated TiO_2 band gap found for the three slab models is approximately 2 eV, the experimental value of 3.2 eV is underestimated in pure DFT methods. It can be observed that for the three dopamine adsorption systems a state is present in the middle of the TiO_2 band gap. This state is localized on the molecule and corresponds to the one observed in cluster models too^{20,21}. Interestingly, catechol adsorption on TiO_2 (101) also displays a molecular state in the gap for the molecular and monodentate modes³⁶. For lower energies it is found that the valence band of the slab is mainly formed by oxygen p states, whereas for higher energies the conduction band is mainly composed of Ti 3d empty states.

A comparison of the three terminations shows that in the (001) adsorption system the molecular level is closer to the conduction band than for either the (100) or the (101) slabs. Although the analysis is not quantitative, this might be connected to a better coupling of the molecule with this surface, and is consistent with the high adsorption energy found for this system. In the three cases studied the excited states of the molecule do not lie in the lower part of the conduction band, but at higher energy (for instance in the (001) system dopamine states lie 2 eV and 4 eV above the Fermi energy). This might be an indication of a direct photoionization mechanism without the intervention of an intermediate excited state as has been proposed in the literature for catechol¹⁵. In the direct photoionization mechanism the molecular excited states lie within the conduction band, mixed with the host electronic states. In order to check if the electronic structure is influenced by the inherent

problems of pure GGA functionals, we have calculated the DOS of the three structures with PBE+U ($U-J=4$); the plots are displayed in Supporting information. The main change observed correspond to a shift to higher energies of the bottom of the conduction band, as expected from the inclusion of the $U-J=4$ for Ti 3d levels, and the band gap is therefore increased. The presence of a molecular state in the gap as well as the mixing of molecular excited states with the TiO_2 conduction band is preserved when including the Hubbard correction.

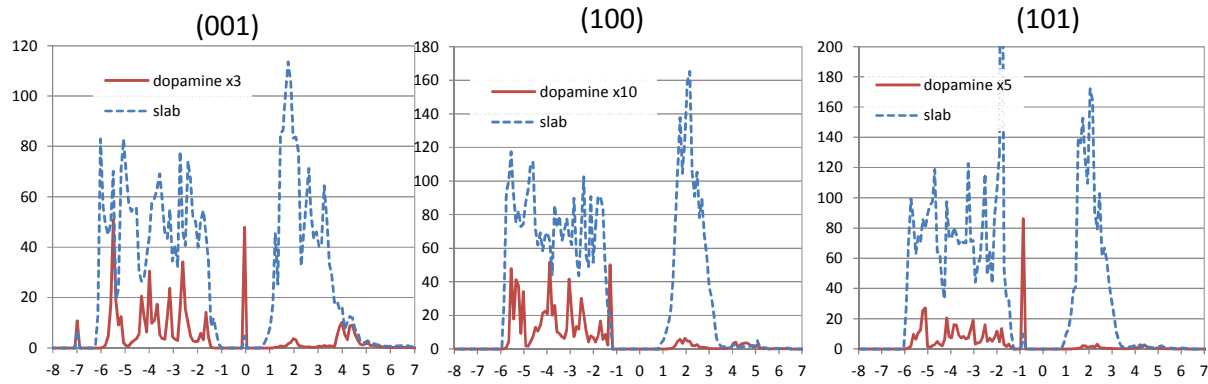


Figure 2: dopamine and slab-projected DOS for the three terminations of anatase calculated at the PBE level, models shown in Figure 1. The Fermi level is shifted to the zero energy. y axis: DOS in arbitrary units, x axis: energy in eV.

In order to mimic the excitation by a laser field the triplet states of the three adsorption systems selected have been calculated. In these excited states the optimized geometry is kept fixed and one electron is promoted to the conduction band, keeping the difference between alpha and beta electrons equal to 2. The calculated singlet-triplet energy gap is given in Table 3 for the GGA and GGA+U calculations. The (001) slab model shows the narrowest gap, followed by (100) and (101) models. Also it can be observed that the GGA+U values are larger than the pure GGA values, as expected from the inclusion of the Hubbard parameter on the Ti 3d states, but with same trends as regards the surface termination.

	GGA	GGA+U
(001)	1.82	1.96
(100)	1.91	2.10
(101)	1.94	2.20

Table 3: Singlet-triplet gap obtained for GGA and GGA+U ($U-J=4$ eV), in eV.

The visualization of the $N_{\alpha-\beta}$ spin density in the triplet state is shown in Figure 3 for the three systems. In this representation the isosurface of the $N_{\alpha-\beta}$ spin density is centered on the molecule (aromatic ring and oxygen sites bonded to the surface) as well as on a single surface titanium site, as corresponds to the occupation of both the HOMO and LUMO states by one electron each. This picture supports a charge transfer mechanism that would take place from the molecule to the surface resulting in an increase of the transition dipole moment.

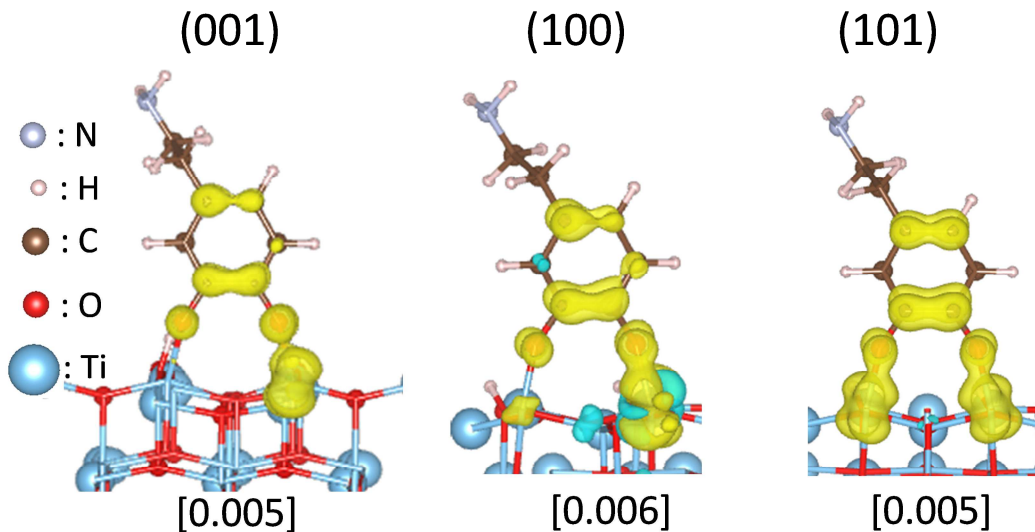


Figure 3: the spin localization in the triplet state for the dopamine adsorbed on the three anatase slabs. The spin isosurfaces are displayed in yellow. In square brackets the isocontour values in $\text{eV}/\text{\AA}^3$. The Vesta program³⁷ has been used for visualization.

Bader population analysis has been carried out for the spin density of the triplet states at the GGA+U level, and is summarized in Table 4. It can be seen that upon excitation from the singlet to the triplet state the contribution of the dopamine fragment is 0.84/0.93, essentially localized at the aromatic ring (0.47/0.60) and on the oxygen atoms (0.14/0.21). The slab's contribution accounts for the rest, 1.06/1.12, essentially localized on the Ti surface sites bonded to the dopamine. Note that for the model (100) the two Ti sites bonded to the molecule possess a similar spin density, 0.45/0.53, whereas for the (001) and (101) one titanium site concentrates the spin, 0.11/0.84 and 0.13/0.83 respectively. This spin distribution is again consistent with the charge transfer mechanism responsible of the SERS effect.

	(001)	(100)	(101)
Dopamine	0.87	0.93	0.84
OH groups	0.14/0.21	0.15/0.16	0.16/0.20
Cycle	0.51	0.60	0.47
CH ₂ CH ₂ NH ₂	0.01	0.01	0.00
Slab	1.12	1.06	1.15
Ti-O-C	0.11/0.84	0.53/0.45	0.13/0.83

Table 4: Bader population analysis for the spin density of GGA+U triplet states, computed for selected atoms and groups as in Figure 1.

Conclusions

Collecting all the information above the following statements concerning the dopamine interaction with TiO₂ surfaces we can draw the following conclusions:

- 1) Dopamine adsorption is energetically favorable in the three terminations of bare anatase studied. The molecule deprotonates and binds to two surface titanium sites in a bidentate mode.
- 2) The (001) exhibits a more favorable adsorption energy, -1.82 eV compared to the (100) termination, -1.14 eV. The least favorable adsorption is found for the (101) terminated slab, -0.67 eV. This indicates clearly a preference of the dopamine molecule for the (001) slab.
- 3) Upon adsorption the dopamine molecule forms a charge transfer complex and transfers ~0.7/0.8 electrons to the anatase surface. Also, the electronic structure displays a state in the TiO₂ band gap that corresponds to the molecule (HOMO) whereas the conduction band corresponds to empty titanium 3d states (LUMO). This picture is consistent with a charge transfer mechanism from the molecule to the semiconductor slab.
- 4) Excitation of the system to a triplet state involves the promotion of an electron from the molecule to the surface titanium sites.

Although the models used consider perfect stoichiometric infinite slabs they help to understand the mechanisms of adsorption. The electronic structure of dopamine adsorbed on anatase surfaces explains key experimental results about SERS. The charge transfer mechanism suggested in the literature, involving the excitation of electrons from the molecule to the surface, is supported by our results. Further investigations are needed to

address the role of the solvent, in particular in the protonation of the amine group, as well as the presence of structural (steps, reconstruction) and electronic (titanium reduction) defects in the charge transfer mechanism.

Acknowledgements

This work was financially supported by project NSF-ANR (ANR-11-NS04-0001 FRAMOLENT program). This work was performed using HPC resources from GENCI- CINES/IDRIS (Grants 2012-x2012082131, 2013-x2013082131, 2014-x2014082131) and the CCRE-DSI of Université P. M. Curie. Dr. B. Diawara is warmly acknowledged for the Modelview visualization program. We would like to acknowledge also Dr. Enrique Poulain at FAMA, UAM unidad Azcapotzalco, Mexico, for the facilities. DFS acknowledges Research in Paris program for a postdoctoral grant.

Supporting Information Available

Optimized structures for dopamine adsorbed on (001), (100) and (101) anatase slabs.

Table S1: atomic Bader charges of the gas-phase molecule and differences between the gas-phase and the adsorbed molecule.

Figure S1: slab and dopamine projected DOS obtained with PBE+U (U-J=4).

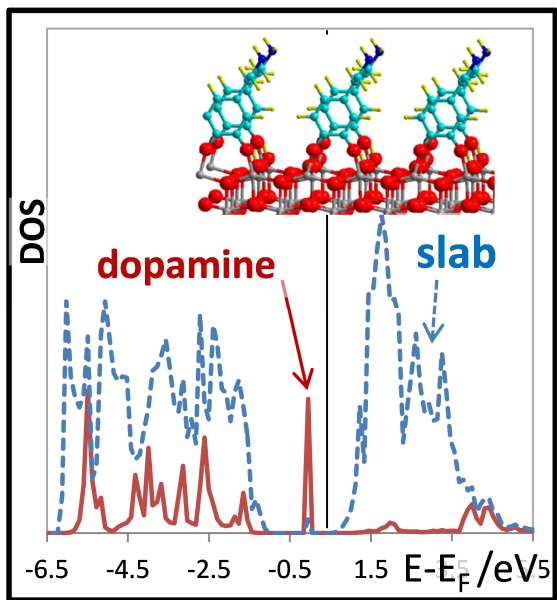
This material is available free of charge via the Internet at <http://pubs.acs.org>

References

- (1) Chen, X.; Mao, S. S. Titanium Dioxide Nanomaterials: Synthesis, Properties, Modifications, and Applications *Chem. Rev.* **2007**, *107*, 2891-2959.
- (2) Linsebigler, A. L.; Lu, G.; Yates, J. T. Photocatalysis on TiO₂ Surfaces: Principles, Mechanisms, and Selected Results *Chem. Rev.* **1995**, *95*, 735-758.
- (3) Finkelstein-Shapiro, D.; Tarakeshwar, P.; Rajh, T.; Mujica, V. Photoinduced Kinetics of Sers in Bionorganic Hybrid Systems. A Case Study: Dopamine-TiO₂ *J. Phys. Chem. B* **2010**, *114*, 14642-14645.
- (4) Musumeci, A.; Gosztola, D.; Schiller, T.; Dimitrijevic, N. M.; Mujica, V.; Martin, D.; Rajh, T. SERS of Semiconducting Nanoparticles (TiO₂ Hybrid Composites) *J. Am. Chem. Soc.* **2009**, *131*, 6040-6041.
- (5) Yang, L.; Jiang, X.; Ruan, W.; Zhao, B.; Xu, W.; Lombardi, J. R. Adsorption Study of 4-MBA on TiO₂ Nanoparticles by Surface-Enhanced Raman Spectroscopy *J. Raman Spectrosc.* **2009**, *40*, 2004-2008.
- (6) Pérez Leon, C.; Kador, L.; Peng, B.; Thelakkat, M. Characterization of the Adsorption of Ru-Bpy Dyes on Mesoporous TiO₂ Films with UV-Vis, Raman, and FTIR Spectroscopies *J. Phys. Chem. B* **2006**, *110*, 8723-8730.
- (7) Quagliano, L. G. Observation of Molecules Adsorbed on III-V Semiconductor Quantum Dots by Surface-Enhanced Raman Scattering *J. Am. Chem. Soc.* **2004**, *126*, 7393-7398.
- (8) Hayashi, S.; Koh, R.; Ichiyama, Y.; Yamamoto, K. Evidence for Surface-Enhanced Raman Scattering on Nonmetallic Surfaces: Copper Phthalocyanine Molecules on Gap Small Particles *Phys. Rev. Lett.* **1988**, *60*, 1085-1088.
- (9) Yamada, H.; Yamamoto, Y.; Tani, N. Surface-Enhanced Raman Scattering (SERS) of Adsorbed Molecules on Smooth Surfaces of Metals and a Metal Oxide *Chem. Phys. Lett.* **1982**, *86*, 397-400.
- (10) Shoute, L. C. T.; Loppnow, G. R. Excited-State Dynamics of Alizarin-Sensitized TiO₂ Nanoparticles from Resonance Raman Spectroscopy *J. Chem. Phys.* **2002**, *117*, 842-850.
- (11) Wang, Y.; Hang, K.; Anderson, N. A.; Lian, T. Comparison of Electron Transfer Dynamics in Molecule-to-Nanoparticle and Intramolecular Charge Transfer Complexes *J. Phys. Chem. B* **2003**, *107*, 9434-9440.
- (12) Syres, K.; Thomas, A.; Bondino, F.; Malvestuto, M.; Grätzel, M. Dopamine Adsorption on Anatase TiO₂(101): A Photoemission and NEXAFS Spectroscopy Study *Langmuir* **2010**, *26*, 14548-14555.
- (13) Syres, K. L.; Thomas, A. G.; Flavell, W. R.; Spencer, B. F.; Bondino, F.; Malvestuto, M.; Preobrajenski, A.; Grätzel, M. Adsorbate-Induced Modification of Surface Electronic Structure: Pyrocatechol Adsorption on the Anatase TiO₂ (101) and Rutile TiO₂ (110) Surfaces *J. Phys. Chem. C* **2012**, *116*, 23515-23525.
- (14) Sanchez-de-Armas, R.; San-Miguel, M. A.; Oviedo, J.; Marquez, A.; Sanz, J. F. Electronic Structure and Optical Spectra of Catechol on TiO₂ Nanoparticles from Real Time TD-DFT Simulations *Phys. Chem. Chem. Phys.* **2011**, *13*, 1506-1514.
- (15) Xu, Y.; Chen, W.-K.; Liu, S.-H.; Cao, M.-J.; Li, J.-Q. Interaction of Photoactive Catechol with TiO₂ Anatase (101) Surface: A Periodic Density Functional Theory Study *Chem. Phys.* **2007**, *331*, 275-282.
- (16) Nawrocka, A.; Zdyb, A.; Krawczyk, S. Stark Spectroscopy of Charge-Transfer Transitions in Catechol-Sensitized TiO₂ Nanoparticles *Chem. Phys. Lett.* **2009**, *475*, 272-276.
- (17) Liu, Y.; Dadap, J. I.; Zimdars, D.; Eisenthal, K. B. Study of Interfacial Charge-Transfer Complex on TiO₂ Particles in Aqueous Suspension by Second-Harmonic Generation *J. Phys. Chem. B* **1999**, *103*, 2480-2486.
- (18) Liu, L.-M.; Li, S.-C.; Cheng, H.; Diebold, U.; Selloni, A. Growth and Organization of an Organic Molecular Monolayer on TiO₂: Catechol on Anatase (101) *J. Am. Chem. Soc.* **2011**, *133*, 7816-7823.
- (19) Li, S.-C.; Losovyj, Y.; Diebold, U. Adsorption-Site-Dependent Electronic Structure of Catechol on the Anatase TiO₂(101) Surface *Langmuir* **2011**, *27*, 8600-8604.

- (20) Tarakeshwar, P.; Finkelstein-Shapiro, D.; Hurst, S. J.; Rajh, T.; Mujica, V. Surface-Enhanced Raman Scattering on Semiconducting Oxide Nanoparticles: Oxide Nature, Size, Solvent, and pH Effects *J. Phys. Chem. C* **2011**, *115*, 8994-9004.
- (21) Tarakeshwar, P.; Finkelstein-Shapiro, D.; Rajh, T.; Mujica, V. Quantum Confinement Effects on the Surface Enhanced Raman Spectra of Hybrid Systems Molecule-TiO₂ Nanoparticles *Int. J. Quantum. Chem.* **2011**, *111*, 1659-1670.
- (22) Vega-Arroyo, M.; LeBreton, P. R.; Rajh, T.; Zapol, P.; Curtiss, L. A. Density Functional Study of the TiO₂-Dopamine Complex *Chem. Phys. Lett.* **2005**, *406*, 306-311.
- (23) Tarakeshwar, P.; Palma, J. L.; Finkelstein-Shapiro, D.; Keller, A.; Urdaneta, I.; Calatayud, M.; Atabek, O.; Mujica, V. SERS as a Probe of Charge-Transfer Pathways in Hybrid Dye/Molecule-Metal Oxide Complexes *J. Phys. Chem. C* **2014**, *118*, 3774-3782.
- (24) Urdaneta, I.; Pilme, J.; Keller, A.; Atabek, O.; Tarakeshwar, P.; Mujica, V.; Calatayud, M. Probing Raman Enhancement in a Dopamine-Ti₂O₄ Hybrid Using Stretched Molecular Geometries *J. Phys. Chem. A* **2014**, *118*, 1196-1202.
- (25) Kresse, G.; Furthmüller, J. Efficient Iterative Schemes for Ab Initio Total-Energy Calculations Using a Plane-Wave Basis Set *Phys. Rev. B* **1996**, *54*, 11169-11186.
- (26) Kresse, G.; Hafner, J. Ab Initio Molecular Dynamics for Open-Shell Transition Metals *Phys. Rev. B* **1993**, *48*, 13115-13118.
- (27) Perdew, J. P.; Burke, K.; Ernzerhof, M. Generalized Gradient Approximation Made Simple *Phys. Rev. Lett.* **1996**, *77*, 3865-3868.
- (28) Blochl, P. E. Projector Augmented-Wave Method *Phys. Rev. B* **1994**, *50*, 17953-17979.
- (29) Kresse, G.; Joubert, D. From Ultrasoft Pseudopotentials to the Projector Augmented-Wave Method *Phys. Rev. B* **1999**, *59*, 1758-1775.
- (30) Redfern, P. C.; Zapol, P.; Curtiss, L. A.; Rajh, T.; Thurnauer, M. C. Computational Studies of Catechol and Water Interactions with Titanium Oxide Nanoparticles *J. Phys. Chem. B* **2003**, *107*, 11419-11427.
- (31) Beltran, A.; Sambrano, J. R.; Calatayud, M.; Sensato, F. R.; Andrés, J. Static Simulation of Bulk and Selected Surfaces of Anatase TiO₂ *Surf. Sci.* **2001**, *490*, 116-124.
- (32) Barnard, A. S.; Curtiss, L. A. Prediction of TiO₂ Nanoparticle Phase and Shape Transitions Controlled by Surface Chemistry *Nano Lett.* **2005**, *5*, 1261-1266.
- (33) Calatayud, M.; Minot, C. Effect of Relaxation on Structure and Reactivity of Anatase (100) and (001) Surfaces *Surf. Sci.* **2004**, *552*, 169-179.
- (34) Henkelman, G.; Arnaldsson, A.; Jonsson, H. A Fast and Robust Algorithm for Bader Decomposition of Charge Density *Comput. Mat. Sci.* **2006**, *36*, 354-360.
- (35) Calatayud, M.; Markovits, A.; Menetrey, M.; Mguig, B.; Minot, C. Adsorption on Perfect and Reduced Surfaces of Metal Oxides *Catal. Today* **2003**, *85*, 125-143.
- (36) Di Valentin, C.; Fittipaldi, D. Hole Scavenging by Organic Adsorbates on the TiO₂ Surface: A DFT Model Study *J. Phys. Chem. Lett.* **2013**, *4*, 1901-1906.
- (37) Momma, K.; Izumi, F. Vesta: A Three-Dimensional Visualization System for Electronic and Structural Analysis *J. Appl. Crystall.* **2008**, *41*, 653-658.

TOC image



Dopamine Adsorption on TiO₂ Anatase Surfaces.

I. Urdaneta, A. Keller, O. Atabek, J. L. Palma, D. Finkelstein-Shapiro, T. Pilarisetty, V. Mujica, M. Calatayud

Supporting Information

- Files containing the geometry of the most stable systems found for the slabs in interaction with dopamine
- Table S1 : Bader charges in gas-phase dopamine molecule, and charge difference ($q_{\text{adsorbed}} - q_{\text{gas-phase}}$), in |e|. Positive values indicate atoms that transfer electrons upon adsorption, negative values those that withdraw electrons upon adsorption.
- Figure S1: slab and dopamine projected DOS obtained with PBE+U (U-J=4).

Files containing the geometry of the most stable systems found for the slabs in interaction with dopamine

Dopamine adsorbed on (001) slab Eads = -1.86 eV						
1.000000000000000						
7.570000000000003	0.000000000000000	0.000000000000000				
0.000000000000000	7.570000000000003	0.000000000000000				
0.000000000000000	0.000000000000000	40.000000000000000				
O Ti H N C						
50 24 11 1 8						
Selective dynamics						
Direct						
0.5410812709345922	0.4912348316847168	0.4999799812928405	T	T	T	
0.9853151247286903	0.5001882102285834	0.4943785538073432	T	T	T	
0.9849740453686494	0.0015950216430137	0.4944238906093129	T	T	T	
0.5408857793728136	0.0092477692225398	0.4999510494577226	T	T	T	
0.2564276484018472	0.2510771485942941	0.4766719062087973	T	T	T	
0.2576728804942346	0.7514499805232426	0.4736331406837849	T	T	T	
0.7507155225900847	0.7504849325294251	0.4686682831597785	T	T	T	
0.7548642606944462	0.2506274867480301	0.4680556306415990	T	T	T	
0.2474790488036288	0.0020657903534778	0.4364550687765034	T	T	T	
0.7509373162325716	0.5009471019983638	0.4288493841236214	T	T	T	
0.7512893967600918	0.0002286143683327	0.4288548806596346	T	T	T	
0.2475993336506230	0.5002583213757347	0.4365338263386049	T	T	T	
0.4974743931250677	0.7508972799752113	0.4102901628688920	T	T	T	
0.005077445058151	0.2512080365760957	0.4105784952194041	T	T	T	
0.4980542934962254	0.2508208293913697	0.4107140387917786	T	T	T	
0.0044280197486030	0.7505601749615152	0.4103815108352383	T	T	T	
0.2513700633098677	0.7500076860834347	0.3714977961493572	T	T	T	
0.7510836695261891	0.7499350290549693	0.3698125714113277	T	T	T	
0.2519605009814286	0.2500123921239317	0.3724202376394319	T	T	T	
0.7514846957516879	0.2499297849704782	0.3697374227758068	T	T	T	
0.0033196065964606	0.0002251057928155	0.3490250361628436	T	T	T	
0.4989073259299128	0.0002086919072544	0.3488338676261379	T	T	T	
0.0033021909612403	0.4998185923356428	0.3489848738483767	T	T	T	
0.4989057310260526	0.4998642196241517	0.3488416518019367	T	T	T	
0.0052665453399693	0.7500463258152646	0.3095841783452060	T	T	T	
0.0080355819772201	0.2499813121666761	0.3096800781368876	T	T	T	
0.5008982834556545	0.2500360128342376	0.3096261979045115	T	T	T	
0.5031945940605695	0.7500082272845324	0.3094391252878699	T	T	T	
0.2538579026081869	0.5009538324375564	0.2870779836457306	T	T	T	
0.7538711118162927	0.0014564902467318	0.2873340980088170	T	T	T	
0.7539037712260798	0.4988071494624038	0.2873404179248584	T	T	T	
0.2538265028153351	0.9992832244603652	0.2870855653766036	T	T	T	
0.5047930688913105	0.0000717229756939	0.2481261882763200	T	T	T	
0.0045189862335564	0.4996100594000688	0.2482391983703550	T	T	T	
0.0045239320764443	0.9993584893656347	0.2482582784850509	T	T	T	
0.5048280214484508	0.4990843682692782	0.2481552554116371	T	T	T	
0.2679506126318069	0.2497797376374511	0.2257708513862139	T	T	T	
0.7680184678971405	0.7497710804943547	0.2258462116254533	T	T	T	
0.7685976462146349	0.2497494304445290	0.2257603294823974	T	T	T	
0.2685514511923709	0.7497643534961637	0.2257581679168078	T	T	T	
0.2242459966146884	0.9997816447712375	0.1870599562053996	T	T	T	
0.2242876185194632	0.499830473111041	0.1870467791198086	T	T	T	
0.7245396652846833	0.4997783259766289	0.1871228459880838	T	T	T	
0.7245543054872241	0.9998262792721705	0.1871193296311427	T	T	T	
0.9767694177030212	0.7498584920880502	0.1622646136426772	T	T	T	
0.9768185608367492	0.2498357529533492	0.1621885958701458	T	T	T	
0.4770715780374833	0.7498638365405509	0.1622451053714913	T	T	T	
0.4769097531915343	0.2498308529835390	0.1622438931742103	T	T	T	

0.2596455795799565	0.5634103903852434	0.5335435484650899	T	T	T
0.2591385544695129	0.9429094569248366	0.5338751654953919	T	T	T
0.2288051246242458	0.5044296003282760	0.4882099782306357	T	T	T
0.7622537829072584	0.0012531799322862	0.4772426726662133	T	T	T
0.2288842375835982	0.9982676486813783	0.4883665637656190	T	T	T
0.7622896372752291	0.4997664081408779	0.4772203002523417	T	T	T
0.2525581678140050	0.2508937666811308	0.4250105456836990	T	T	T
0.2513246818726208	0.7512623609932686	0.4240813984053204	T	T	T
0.7518700987184580	0.2505641489398781	0.4185217923025926	T	T	T
0.7504359850864586	0.7505838545138989	0.4186231899127647	T	T	T
0.0061943833097546	0.7500132922157730	0.3599452860158047	T	T	T
0.4963394944512444	0.2500296193411625	0.3600203706433545	T	T	T
0.4963905760664183	0.7500298378330640	0.3597400673044105	T	T	T
0.0073260276883919	0.2500422097220009	0.3602022117044459	T	T	T
0.5036027239864854	0.4997748750443629	0.2984001152502179	T	T	T
0.0037556773995771	0.0001803061455423	0.2985501285297940	T	T	T
0.0037599366754765	0.4997763224866457	0.2985420227350680	T	T	T
0.5035862356692686	0.0002046738777008	0.2983980474181120	T	T	T
0.2508722485793052	0.9997569406885313	0.2366823481602293	T	T	T
0.2508931462824948	0.4998096167687090	0.2366824088613113	T	T	T
0.7511277132539589	0.9999103830720399	0.2366935985096410	T	T	T
0.7511519765079870	0.4996496536595187	0.2366912153099123	T	T	T
0.2540460805570236	0.7498161398627041	0.1770178251880118	T	T	T
0.7539456969508720	0.249809647446715	0.1770142220548185	T	T	T
0.2539108263144754	0.2498186844055860	0.1770155302922877	T	T	T
0.7538620997302760	0.7498118775015048	0.1770634693410975	T	T	T
0.2596969554592984	0.4234793663697106	0.5915057060512438	T	T	T
0.2658576473961899	0.9136795386925884	0.6466275678318141	T	T	T
0.2616997259526071	0.0785201715575668	0.5927030620350864	T	T	T
0.3289836102235920	0.4271754264868526	0.6527645594699549	T	T	T
0.3185054305709549	0.6279191059791098	0.6755260275088041	T	T	T
0.0029687221020264	0.4308794280671738	0.6450484280338049	T	T	T
0.9891722582968361	0.6338923895745073	0.6669652970518238	T	T	T
0.1081353582106278	0.4740560095606469	0.7155585068333480	T	T	T
0.9341724227427916	0.3678828857399964	0.7017226489684990	T	T	T
0.5238767581685227	0.9786179204299879	0.5234063438299925	T	T	T
0.5235016804867715	0.5284547059620968	0.5230839551013693	T	T	T
0.0612402603434914	0.4017214575273753	0.6958253503873748	T	T	T
0.2630864846129543	0.8412853218787401	0.6230016441361198	T	T	T
0.2597216568928695	0.5678130018419995	0.5924684379210936	T	T	T
0.2625820407435518	0.6558674850339163	0.6231347420086762	T	T	T
0.2605761332718179	0.9343539306066694	0.5930119316998159	T	T	T
0.2572732278490579	0.6580091244664806	0.5617912399483737	T	T	T
0.2573091197429902	0.8470580182955403	0.5619903913727347	T	T	T
0.2553031051323174	0.5520717651194406	0.6552155457822798	T	T	T
0.0645790598956943	0.5085715673648239	0.6652392160518936	T	T	T

Dopamine adsorbed on (100) slab Eads = -1.14 eV

1.00000000000000
 7.570000000000003 0.0000000000000000 0.0000000000000000
 0.0000000000000000 9.515000000000006 0.0000000000000000
 0.0000000000000000 0.0000000000000000 40.0000000000000000

O Ti H N C

66 32 11 1 8

Selective dynamics

Direct

0.7488293118832607	0.3357943529080864	0.4147642649163776	T	T	T
0.2496231309279575	0.3336925515954481	0.4036623291210138	T	T	T
0.0005667848561121	0.1615603969098638	0.4138542496439523	T	T	T
0.4972713317996245	0.1610187271770639	0.4140517281070510	T	T	T

0.7496727883075276	0.9308158718965159	0.4085245149413794	T	T	T
0.9922460433425064	0.5838783750192581	0.4102580562433564	T	T	T
0.2486910330586410	0.9269093924610725	0.4080675340153739	T	T	T
0.5000270386216983	0.5848010654682311	0.4105319553942811	T	T	T
0.2481938053797972	0.6648258431700417	0.3622150647688999	T	T	T
0.4987880984162040	0.8342579965847561	0.3609202584961321	T	T	T
0.7479060100340923	0.6685628957456583	0.3613787167292305	T	T	T
0.9977467979501422	0.8341733364650891	0.3609044586765929	T	T	T
0.7479908396503676	0.0949092051558700	0.3590796399915493	T	T	T
0.2493485751744321	0.0880016981546185	0.3581923747634295	T	T	T
0.9920127701959415	0.4173706749792410	0.3620284839441368	T	T	T
0.5113948895153141	0.4172744654119537	0.3621277543304250	T	T	T
0.7492515581777879	0.9195376635503293	0.3121216730346510	T	T	T
0.4951726865337748	0.5838952398237158	0.3129233805677507	T	T	T
0.2490098910070622	0.9176107332791348	0.3115568134233381	T	T	T
0.0004192018886732	0.5842280390430289	0.3128763495572905	T	T	T
0.7500489889219857	0.3351515054495969	0.3119100611353610	T	T	T
0.2500548724668518	0.3347746840058572	0.3135751413775928	T	T	T
0.4995777624663513	0.1664282060844119	0.3109569512745972	T	T	T
-0.0000856916410787	0.1664314723642072	0.3110959555231001	T	T	T
0.9989231068545458	0.8317982024653607	0.2632126650682954	T	T	T
0.4996730778424185	0.8318522914543893	0.2632296811882862	T	T	T
0.7491589249205556	0.6632500348235176	0.2652488133110723	T	T	T
0.2492548509789741	0.6636489090590270	0.2642668673038472	T	T	T
0.7499634037748690	0.0835018750592231	0.2622953934466395	T	T	T
0.4987632444210577	0.4142199553819125	0.2642115493133919	T	T	T
0.0019742676840714	0.4142645846985249	0.2642019522061209	T	T	T
0.2493843086166418	0.0838387303656772	0.2621145162368795	T	T	T
0.7494826110748238	0.9130907759039293	0.2153793219822052	T	T	T
0.5010293218252611	0.5827070761384613	0.2161146691636413	T	T	T
0.9976113958213302	0.5826567838234938	0.2160880319607601	T	T	T
0.2496671780678201	0.9135330273823654	0.2152023257748074	T	T	T
0.2499330056360913	0.3316927510119134	0.2153684830925342	T	T	T
0.7499489160269583	0.3313036399228553	0.2157975146174560	T	T	T
0.9998582671717222	0.1637230999357330	0.2135318333768101	T	T	T
0.4999378465896060	0.1636969700591005	0.2135960471128014	T	T	T
0.9997268918123702	0.8304312822695217	0.1672415662505864	T	T	T
0.4997297175311357	0.8304158958186614	0.1672313957562070	T	T	T
0.7496545246824101	0.6606303764333441	0.1676578838704789	T	T	T
0.2497086352457331	0.6603350251598953	0.1680204351406280	T	T	T
0.9996590951978435	0.4149856150348410	0.1668340811868662	T	T	T
0.7498600419427341	0.0772731177350622	0.1655143678100099	T	T	T
0.5004028220578448	0.4150053723773017	0.1668426943879108	T	T	T
0.2499749443749386	0.0773458538000695	0.1653791823336966	T	T	T
0.2498630010520980	0.9013115970533100	0.1183999312759414	T	T	T
0.4991611765353707	0.5890493444072858	0.1189592382917565	T	T	T
0.0003878223682080	0.5890277393878716	0.1189657810634915	T	T	T
0.7498565851816545	0.9015009680627962	0.1184483454903750	T	T	T
-0.0000381725574461	0.1612996705558090	0.1165758332025486	T	T	T
0.2499946532592623	0.3282331720989894	0.1176158145166939	T	T	T
0.4999856611707904	0.1613184009473074	0.1165755649115548	T	T	T
0.7499970391791290	0.3282971192816167	0.1176072396354262	T	T	T
0.7500098008296999	0.0653185926958905	0.0691785474915357	T	T	T
0.5000862874932007	0.4221505591177442	0.0702570904751420	T	T	T
-0.0000003508668530	0.4221543893308175	0.0702545019433828	T	T	T
0.2499994595936791	0.0653287688023013	0.0691306651493290	T	T	T
0.2499461887824659	0.6565611279713921	0.0645139175801889	T	T	T
-0.0001023691643313	0.8306652603599051	0.0641734558270157	T	T	T
0.7499529962266229	0.6565017039285509	0.0646474029357046	T	T	T
0.4999933715309726	0.8306829481865471	0.0641693999311926	T	T	T
0.0570156828845642	0.3880486975051184	0.4596265818402949	T	T	T

0.4409016254060502	0.3885879077980474	0.4599204726175765	T	T	T
0.0057434244060104	0.3745366252528227	0.4144657261059949	T	T	T
0.7485978744104846	0.1241917671681753	0.4039069674472167	T	T	T
0.4951837434435547	0.3749500576213839	0.4148904346637952	T	T	T
0.2492701290879187	0.1212267116201526	0.4027120148470827	T	T	T
0.7481074044750655	0.8786171850571521	0.3628780683058692	T	T	T
0.2482898737874961	0.8748144210791304	0.3627896744475143	T	T	T
0.9958949772720358	0.6213840004474094	0.3600454404494990	T	T	T
0.4982180460087349	0.6209429941634820	0.3601238116275278	T	T	T
-0.0000081791285425	0.3755868019026660	0.3145390065942610	T	T	T
0.7498412509189700	0.1240028387945557	0.3083554431484744	T	T	T
0.5003632771365794	0.3755417352066776	0.3146882648752193	T	T	T
0.2498612748877894	0.1228539555748337	0.3081515574848158	T	T	T
0.7491681512898843	0.873710009415228	0.2649254219990954	T	T	T
0.4993060022119135	0.6175461502228362	0.2643396947860118	T	T	T
0.2492182595549223	0.8732857468421297	0.2646671844952378	T	T	T
0.9993184208215211	0.6177044445582162	0.2643032187546640	T	T	T
-0.00000773978836660	0.3735655769351969	0.2154861013518257	T	T	T
0.5000284615795958	0.3735978199496134	0.2155575092950715	T	T	T
0.2499047893653705	0.1202422732146331	0.2121309774284480	T	T	T
0.7499096740288888	0.1199649523504813	0.2123155349024199	T	T	T
0.7496653131914843	0.8713931423617308	0.1686145798066874	T	T	T
0.4998161852912366	0.6168046704756921	0.1687594482544239	T	T	T
0.9995384974337927	0.6169222479297010	0.1687454806594701	T	T	T
0.2497631363755386	0.8711906635931258	0.1685273554411413	T	T	T
0.2499980139142297	0.1177056974897578	0.1143473463707170	T	T	T
-0.0000055424950511	0.3716268623450233	0.1158206274445751	T	T	T
0.5000024613702169	0.3716606112738927	0.1158304806369898	T	T	T
0.7499797926961747	0.1176516670036499	0.1143792426776087	T	T	T
0.4998375826067833	0.6145777396249397	0.0736363998135737	T	T	T
0.2499391840227842	0.8725293441447824	0.0731894572239802	T	T	T
0.7499113596124470	0.8724796691713255	0.0732430173730238	T	T	T
-0.0000003407417978	0.6145908223987437	0.0736365862047593	T	T	T
0.9196042735915153	0.3427314685092523	0.5162735760680029	T	T	T
0.4096876047982128	0.3023340745289627	0.5706352315901143	T	T	T
0.5741302605194196	0.3436867894305908	0.5175949450696671	T	T	T
0.9280081396228247	0.2409339543667698	0.5754088429135527	T	T	T
0.1274440546433356	0.2508334948172052	0.5985200291554615	T	T	T
0.9077929012956861	0.5015578881502536	0.5739319640924071	T	T	T
0.1101685068132217	0.5153436282026076	0.5959515458136793	T	T	T
0.9607512471941601	0.3946095673927953	0.6423788910163388	T	T	T
0.8411816912361459	0.5305126954369347	0.6313391360021933	T	T	T
0.4437184554125087	0.6485093602571254	0.4263193888395501	T	T	T
0.9543566466606919	0.6516661451686169	0.4269927935228169	T	T	T
0.8845388380164626	0.4342471046716668	0.6234461795555620	T	T	T
0.3370794396780486	0.3203066804924374	0.5474004485642127	T	T	T
0.0638676611561296	0.3428474813644362	0.5173617304335153	T	T	T
0.1515816284123700	0.3199243932109330	0.5475678848447180	T	T	T
0.4299309238271550	0.3435146769243264	0.5179328548202058	T	T	T
0.1539376242916326	0.3667258941577823	0.4872195146033254	T	T	T
0.3428451993146440	0.3671936403626337	0.4873963487261449	T	T	T
0.0472973691626163	0.3051583465894127	0.5794482902701120	T	T	T
0.9904504854089421	0.4493086529412770	0.5929106931334628	T	T	T

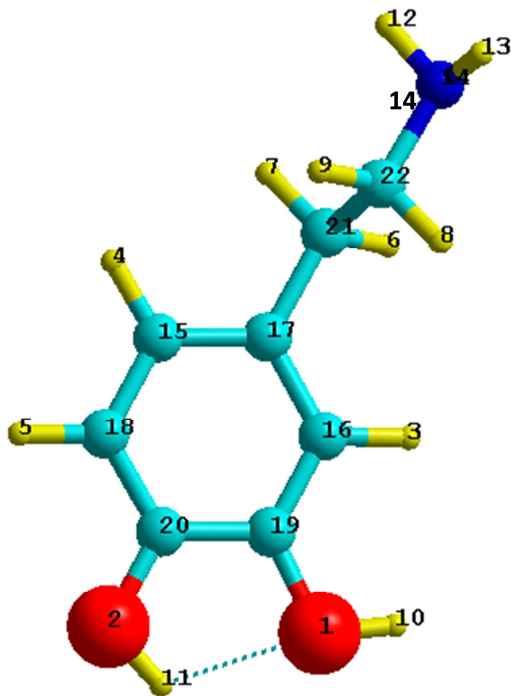
Dopamine adsorbed on (101) slab Eads = -0.67 eV

1.00000000000000	7.570000000000003	0.000000000000000	0.000000000000000	
-3.785000000000001	10.240180000000005	0.000000000000000	0.000000000000000	
0.000000000000000	0.000000000000000	40.000000000000000	0.000000000000000	
O	Ti	H	N	C

66	32	11	1	8			
Selective dynamics							
Direct							
0.1516159301539712	0.8219013207182575	0.3582705463192669	T	T	T		
0.1528904738161633	0.3200015522386127	0.3549792855586585	T	T	T		
0.6629283921756414	0.8236714896013059	0.3586700425838644	T	T	T		
0.6536067298970374	0.3141899048075481	0.3566723499830102	T	T	T		
0.3015619533592092	0.6130188615295286	0.3283698126047209	T	T	T		
0.2971168070953128	0.1042783726549361	0.3419632441680205	T	T	T		
0.7981822263307915	0.1038788573543220	0.3419057124093768	T	T	T		
0.7926004406663090	0.5998536518666826	0.3407197524598308	T	T	T		
0.9805871635177347	0.9697870720018970	0.3186951364914113	T	T	T		
0.4782023183377710	0.9653366976477931	0.3203487277445761	T	T	T		
0.9741674042600726	0.4631116150849617	0.3181668645425842	T	T	T		
0.4758405016760157	0.4616245547414873	0.31979130655564496	T	T	T		
0.1093335118908629	0.7534383674124430	0.2994610001089077	T	T	T		
0.1183273513324398	0.2434042344312540	0.2950358027216703	T	T	T		
0.6165610553730304	0.2433296456266394	0.2959794211199518	T	T	T		
0.6326438367293949	0.7523914207774868	0.2999168596634098	T	T	T		
0.2325497349669998	0.9660804636488115	0.2685319550784206	T	T	T		
0.2266784987899782	0.4584992181315964	0.2660737098622902	T	T	T		
0.7248419107486449	0.9653636825773254	0.2686098489581727	T	T	T		
0.7234305482737404	0.4607544972054881	0.2672263971766503	T	T	T		
0.8694683988639832	0.7477314099155935	0.2460907918378829	T	T	T		
0.3702648605221308	0.2477101261558682	0.2440381303784075	T	T	T		
0.8696857723618693	0.2477556484434748	0.2443424525481780	T	T	T		
0.3681992272668424	0.7448584490792548	0.2481761324422833	T	T	T		
0.5484112633994612	0.6058392896723511	0.2299620778802641	T	T	T		
0.5474761406314290	0.1024639411675041	0.2293086358809459	T	T	T		
0.0459448292764193	0.0999118739530117	0.2294647395819698	T	T	T		
0.0488515344861244	0.6053869166973915	0.2302461717058966	T	T	T		
0.1917660853795632	0.8865337046104528	0.2084874300417885	T	T	T		
0.1904191853387019	0.3898473801580904	0.2060440946085919	T	T	T		
0.6922467893380881	0.3904377789158373	0.2066929131685853	T	T	T		
0.6866399186115960	0.8865659317096024	0.2085436403580053	T	T	T		
0.7993065356176066	0.6050263344056653	0.1779044130015345	T	T	T		
0.7990313702817052	0.1036193515555597	0.1783956548189158	T	T	T		
0.2990336394620710	0.6057439435642479	0.1777611317763653	T	T	T		
0.2974646154885392	0.1034479312828745	0.1783391342109888	T	T	T		
0.4424191479309091	0.3914309075354228	0.1545604475006816	T	T	T		
0.9421984449716091	0.3916610201932041	0.1543960053429171	T	T	T		
0.9409596500286606	0.8890485496524216	0.1566795255018885	T	T	T		
0.4414409243162655	0.8898744926555298	0.1561139496138227	T	T	T		
0.1196338114644034	0.7463441552925365	0.1394196833149464	T	T	T		
0.1187112306085287	0.2442921588012136	0.1406230182192571	T	T	T		
0.6196694898626457	0.7462728915832278	0.1395561865232620	T	T	T		
0.6183984072635346	0.2436329767202367	0.1409458353440193	T	T	T		
0.2621720151875499	0.0322075779192406	0.1177682951663602	T	T	T		
0.7631405261316794	0.0322935481826375	0.1178382796300622	T	T	T		
0.2641205435613311	0.5347345669211530	0.1167162989044017	T	T	T		
0.7630951326834465	0.5342489764708493	0.1168926410633706	T	T	T		
0.8732359612516777	0.2543852323259843	0.0895234577103393	T	T	T		
0.8740068102056864	0.7550883199132034	0.0887438518082762	T	T	T		
0.3746665359633792	0.7551679770588120	0.0885612677466369	T	T	T		
0.3746488137464046	0.2542563074805790	0.0894952085913704	T	T	T		
0.5159683129428461	0.5385473818835677	0.0649712743863082	T	T	T		
0.5155779339349802	0.0375162942411107	0.0659232429955263	T	T	T		
0.0156562131165483	0.0377281438719369	0.0659111605044993	T	T	T		
0.0160007857020687	0.5385974550014533	0.0650689445254023	T	T	T		
0.6952695574417104	0.3969487013141180	0.0446325944869905	T	T	T		
0.1959330698734342	0.8984053041904486	0.0441070908182182	T	T	T		

0.6960395994731455	0.8984966170827823	0.0440537594338132	T	T	T
0.195185393557004	0.3968003366012469	0.0445790808641546	T	T	T
0.8413923136353251	0.1883039424945828	0.0289492563736047	T	T	T
0.8414780546891750	0.6895140109277276	0.0280662630931015	T	T	T
0.3415570908968340	0.1883971072803697	0.0288941305205441	T	T	T
0.3414687212838585	0.6895167251204862	0.0278920137142253	T	T	T
0.4771430249394993	0.5977711780214604	0.3866091575494084	T	T	T
0.0950474402812260	0.5883774113253450	0.3841261752137651	T	T	T
0.0648792901231469	0.6380798254370440	0.3404828318184672	T	T	T
0.0750622457860876	0.1592297691750036	0.3350274215631228	T	T	T
0.5735176263376253	0.1551950284845798	0.3352889277033183	T	T	T
0.5574863154325463	0.6384029828060183	0.3421616685697878	T	T	T
0.2097965233250265	0.9314089824998234	0.3163369834131652	T	T	T
0.2079536269184722	0.4268759544801558	0.3161484850317463	T	T	T
0.7125651952427933	0.9308689142239599	0.3163068559676106	T	T	T
0.7058321258495119	0.4244435585037558	0.3191547487923058	T	T	T
0.1375124212978779	0.7841597234040054	0.2507382514274060	T	T	T
0.1386943099256973	0.2856698454472419	0.2453235417957127	T	T	T
0.6375049969334836	0.7833577721869468	0.2512303151396263	T	T	T
0.6400320024381628	0.2880246620011721	0.2462849008784471	T	T	T
0.2780617621762008	0.0623520814125818	0.2267610782454745	T	T	T
0.2790112396957966	0.5661518659714861	0.2269474703873289	T	T	T
0.7759173005724420	0.0619048919394529	0.2267042391037094	T	T	T
0.7783673399881927	0.5654394851167953	0.2276995449780483	T	T	T
0.2095103428062098	0.9259849326420390	0.1585083643414405	T	T	T
0.7095065704202410	0.9257755957330999	0.1587432041867048	T	T	T
0.2106876874183785	0.4284014723813694	0.1565772826695613	T	T	T
0.7110765253317876	0.4286781044283569	0.1569000394312227	T	T	T
0.3490798909552573	0.7052204927614029	0.1379562930368719	T	T	T
0.8486648607028139	0.7045323912245759	0.1382663986874323	T	T	T
0.8475828783469046	0.2026268172614021	0.1383760006447110	T	T	T
0.3480459165761642	0.2028480307021094	0.1384186462876057	T	T	T
0.7845820654548121	0.0753247409216930	0.0657785444311999	T	T	T
0.7852589588495219	0.5768888406650501	0.0648353554767625	T	T	T
0.2846698424988125	0.0753547730799333	0.0656963104862618	T	T	T
0.2852061490299969	0.5767584368284259	0.0646541293766175	T	T	T
0.9205092534867060	0.8477895379520649	0.0502245604423589	T	T	T
0.4206821885712811	0.8478267640352365	0.0500479163895087	T	T	T
0.9199794794132933	0.3466562697192957	0.0508218054903594	T	T	T
0.4203089069117683	0.3466901051786574	0.0508224484582291	T	T	T
0.6399944345537277	0.6770572471234568	0.4433062464730670	T	T	T
0.1638700645690225	0.7398948210800504	0.4899635186627244	T	T	T
0.9770199835687033	0.6603489569044814	0.4377572915530768	T	T	T
0.6766457971637120	0.8005824343604634	0.4979592968971798	T	T	T
0.4779584715819139	0.8255123201441322	0.5160043198329004	T	T	T
0.5525789346505152	0.5669682023634756	0.5132284494883030	T	T	T
0.3400619615532890	0.5819903829071369	0.5278889274685888	T	T	T
0.5297220562850401	0.7291879699187368	0.5708384062223049	T	T	T
0.5779548978476540	0.5941714810831801	0.5718189943055038	T	T	T
0.1901373163305490	0.8458624766901346	0.3812854810014742	T	T	T
0.6471347467053319	0.8493310636466592	0.3813618373616089	T	T	T
0.5912113402010138	0.6745178060002528	0.5575236721241247	T	T	T
0.2291891940737818	0.7106719660223171	0.4684515903445398	T	T	T
0.4957210662086087	0.6773916324382450	0.4424104449160636	T	T	T
0.4166627034538897	0.7157072542849600	0.4704167171479097	T	T	T
0.1246369677392095	0.6680807898112963	0.4394080632661466	T	T	T
0.3943744833890713	0.6347888030640831	0.4125375639921303	T	T	T
0.2029040725442357	0.6296628641520196	0.4112030890528531	T	T	T
0.5246002818360679	0.7533239165545320	0.5026766027640178	T	T	T
0.4939437984663058	0.6347968834375944	0.5255111456603293	T	T	T

Table S1 : Bader charges in gas-phase dopamine molecule, and charge difference ($q_{\text{adsorbed}} - q_{\text{gas-phase}}$), in $|e|$. Positive values indicate atoms that transfer electrons upon adsorption, negative values those that withdraw electrons upon adsorption.



	q_{gas}	$\Delta q_{001\text{-gas}}$	$\Delta q_{100\text{-gas}}$	$\Delta q_{101\text{-gas}}$
1O	-1.83	0.23	0.27	0.28
2O	-1.82	0.23	0.24	0.24
3H	-0.05	0.03	0.11	0.05
4H	0.04	-0.06	0.01	-0.03
5H	0.04	0.04	-0.03	0.02
6H	0.02	0.02	-0.01	-0.01
7H	-0.06	0.05	0.04	0.07
8H	-0.01	0.04	0.03	0.02
9H	-0.01	0.00	0.01	-0.06
10H	1.00	0.00	0.00	0.00
11H	1.00	0.00	0.00	0.00
12H	1.00	0.00	0.00	0.00
13H	1.00	0.00	0.00	0.00
14N	-2.86	0.00	0.01	0.51
15C	-0.16	0.12	0.13	0.21
16C	0.12	-0.20	-0.11	-0.13
17C	0.12	0.12	-0.14	-0.17
18C	-0.03	-0.07	0.08	0.01
19C	0.67	0.19	0.31	0.26
20C	0.89	0.12	-0.10	0.04
21C	0.04	-0.03	0.02	-0.02
22C	0.89	-0.06	-0.07	-0.48
cycle C6H3	1.64	0.29	0.25	0.27
CH ₂ CH ₂ NH ₂	0.02	0.02	0.05	0.03
OH	-1.66	0.46	0.51	0.52
total	0.00	0.77	0.81	0.82

Figure S1: slab and dopamine projected DOS obtained with PBE+U ($U-J=4$).

